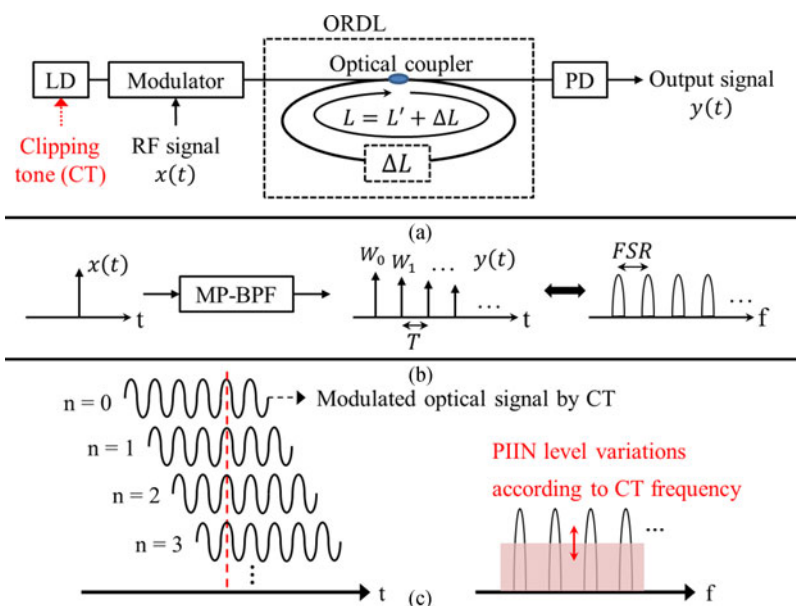


Microwave Photonic Filter Based All-Optical Virtual Private Network Supporting Dynamic Bandwidth Allocation in OFDMA-PON System

Volume 10, Number 1, February 2018

Chang-Hun Kim
Sun-Young Jung
Sang-Kook Han, *Senior Member, IEEE*



DOI: 10.1109/JPHOT.2017.2780198
1943-0655 © 2017 IEEE

Microwave Photonic Filter Based All-Optical Virtual Private Network Supporting Dynamic Bandwidth Allocation in OFDMA-PON System

Chang-Hun Kim , Sun-Young Jung ,
and Sang-Kook Han , *Senior Member, IEEE*

Department of Electrical and Electronic Engineering, Yonsei University, Seoul
07322, South Korea

DOI:10.1109/JPHOT.2017.2780198

1943-0655 © 2017 IEEE. Personal use is permitted, but republication/redistribution requires IEEE permission. See http://www.ieee.org/publications_standards/publications/rights/index.html for more information.

Manuscript received October 13, 2017; revised November 27, 2017; accepted November 30, 2017. Date of publication December 8, 2017; date of current version January 5, 2018. This work was supported by the Institute for Information & communications Technology Promotion (IITP) grant funded by the Korea Government (MSIT) (B0101-17-1276, Access Network Control Techniques for Various IoT Services). Corresponding author: Sang-Kook Han (e-mail: skhan@yonsei.ac.kr).

Abstract: We propose an all-optical virtual private network (VPN) supporting dynamic bandwidth allocation (DBA) in an orthogonal frequency division multiple access-based passive optical network. A microwave photonic bandpass filter (MP-BPF) is used to transmit the VPN signal without electrical conversion. The DBA is implemented by adjusting a free spectral range of the MP-BPF with corresponding subcarrier allocation. A RF clipping-tone (CT) is used to stabilize the optical channel suffered from phase induced-intensity noise and Rayleigh back-scattering noise. The DBA is experimentally verified at different two DBA scenarios in 20-km single-fiber loopback link in terms of channel error vector magnitude, spectral efficiency after adaptive modulation. Due to the CT-based channel stabilization, achievable spectral efficiency could be improved, and the feasibility of the proposed system is successfully demonstrated.

Index Terms: Microwave photonic filter, passive optical network, virtual private network.

1. Introduction

Multi-Carrier parallel transmission has various benefits such as high spectral efficiency, dispersion tolerance, and two dimensional bandwidth allocations in time and frequency domains. For this reason, multi-carrier access based passive optical network (PON) such as OFDMA-PON has been widely researched as a promising candidate for the next generation of optical access requiring fixed mobile convergence, high transmission capacity and bandwidth flexibility [1]–[4]. Such researches have been focused on improvement of transmission capacity, dynamic bandwidth allocation and multiple-access.

On the other hand, all-optical virtual private network (VPN) has been researched to provide virtually dedicated optical channel among optical network units (ONUs) [5]–[10]. In the all-optical VPN system, data traffic among ONUs is transmitted without electrical conversion and electrical processes such as buffer, scheduling and routing algorithms in the OLT through optical relay, while it is suffered from electrical process in the conventional PON system. It is an effective

technique achieving a high throughput, low latency, and better security in optical access, due to data transmission among end users make up high portion of the total traffic. Several types of all-optical VPN in PON system have been reported. In [5], RF subcarrier multiplexing (SCM) is used to transmit VPN data with fiber Bragg gratings (FBG) for optical routing. In [6], it has been demonstrated in two-stage PON architecture using amplitude-shift keying/frequency-shift keying (ASK/FSK) and multiple FBGs. Fabry-Perot laser diode based wavelength conversion effect is used in [7], which requires fine control of optical wavelengths. All-optical VPN is also researched in OFDMA-PON reflecting the recent research trends [8]–[10]. Multi-VPN transmission is demonstrated using subcarrier allocation and wavelength reflector module in [8]. It requires two photodiodes in an ONU to detect VPN and downstream (D/S) data separately. In [9], simulation based intra-VPN and inter-VPN are discussed using comb optical filters with narrow bandwidth. However, most of previously reported all-optical VPN system has low practical feasibility owing to the tight requirements in the optical spectrum, and system complexity, because those systems are based on wavelength sensitive components such as optical filter, FBG with narrow bandwidth [5]–[9]. It has limitations in controlling optical carriers generated from multi-ONUs. Also, additional photodetector (PD) is required in ONU to receive the VPN data separately from conventional data. In our previous work [10], the feasibility of wavelength insensitive all-optical VPN is demonstrated using a microwave photonic bandpass filter (MP-BPF) [11] for the first time. However, it is limited to static VPN system despite of multi-carrier system which has flexibility in bandwidth allocation.

In this paper, tunable MP-BPF based all-optical VPN supporting dynamic bandwidth allocation (DBA) is proposed in multi-carrier access based PON system. It enables to make full use of flexibility in bandwidth allocation. The proposed system is tolerant to optical wavelength, because it uses optical fiber based recirculating delay-line as an optical subsystem for the MP-BPF which is insensitive to wavelength. Also it supports multi-VPN transmission and single-PD operation in ONU. The proposed system has two critical issues should be overcome to improve transmission performance, optical phase induced-intensity noise (PIIN) [11] and multiple access interference (MAI) [3], [4]. A RF clipping-tone (CT) based optical channel stabilization and filter bank multi-carrier (FBMC) [4] are applied to overcome the PIIN and MAI, respectively. The DBA function is experimentally demonstrated in 20-km single fiber loopback link at different two DBA scenarios by adjusting the FSR of MP-BPF with subcarrier allocation. Also, adaptive modulation is applied to verify the achievable spectral efficiency according to the channel variations. The rest of this paper is organized as follows. Section 2 contains basic principle of MP-BPF, CT effect on PIIN, and schematic of proposed all-optical VPN system. In Section 3, experimental setup and results including channel variations and transmission performance according to the CT frequency are discussed. Section 4 concludes our study.

2. Operation Principle and System Schematics

A microwave photonic filter consists of optical transmitter, optical receiver, and optical subsystem as shown in Fig. 1(a). It is used to replace ordinary RF filter, bringing advantages inherent to photonics such as low loss, high bandwidth, adjustability, and immunity to electromagnetic interference. Generally it uses optical fiber based sampling effect, and various type of microwave photonic filter can be designed according to the optical subsystem. The MP-BPF can be designed by using an optical coupler based recirculation delay-line (ORDL) as the optical subsystem as shown in Fig. 1(a). The RF input signal is optically modulated, and fed to ORDL which samples, weights and combines the recirculated signal. Finally, it is converted to electrical signal by a PD. The output signal $y(t)$ can be expressed as (1) where $x(t)$, W_n and T are the input RF signal, tap weight and sampling period, respectively.

$$y(t) = \sum_{n=0}^{N-1} W_n \cdot x(t - nT). \quad (1)$$

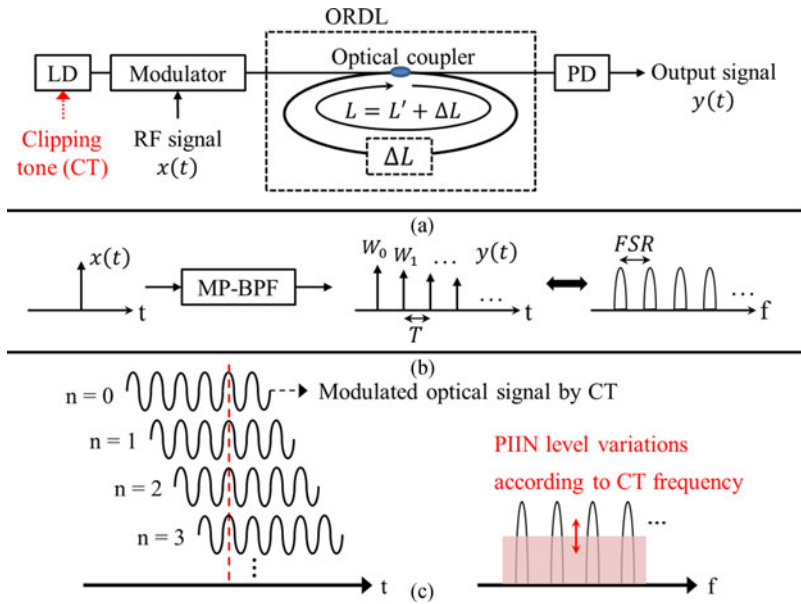


Fig. 1. (a) Layout of MP-BPF, (b) transfer function, and (c) PIIN variations according to CT frequency.

Due to the sampling effect by the ORDL, the MP-BPF has periodic frequency response as shown in Fig 1(b), and the free spectral range (FSR) is decided by the length of delay-line as described in (2) where c , l , and n represent the speed of light, delay-length, and refractive index of fiber, respectively.

$$FSR = \frac{1}{T} = \frac{c}{l \cdot n}. \quad (2)$$

Using this property, tunable MP-BPF could be designed by using an optical tunable delay-line inside of the ORDL. However, the recirculated optical signal leads to intensity noise, because the direct detection transforms the optical phase variations into intensity fluctuation in the incoherent MP-BPF, which is called PIIN [10], [11]. In order to overcome the PIIN, the coherence time of optical source should be much smaller than sampling period of MP-BPF. In our previous work [10], CT modulation based spectrum broadening effect was applied to suppress the PIIN, and the basic structure is shown in Fig. 1(a). The intensity fluctuation by the PIIN could be removed by the spectrum broadening effect. However, the constant noise level according to the applied CT frequency was not investigated. The spectrum broadened optical carrier can be considered as a modulated optical signal by the CT as shown in Fig. 1(c). The PIIN level becomes maximum when the CT frequency corresponds to integer multiple of FSR, because the CT modulated and recirculated optical signals generate the maximum beating noise by the square-law detection as described in Fig. 1(c). On the contrary, the PIIN level could be suppressed by adjusting the CT frequency to be away from the integer multiple of the FSR, and the signal to noise (SNR) of the output signal becomes improved.

Fig. 2 shows the system schematic of the proposed all-optical VPN using MP-BPF. The MP-BPF consists of optical transmitter, optical subsystem, and a receiver as mentioned above. An ONU has a couple of an optical transmitter and a receiver as it of conventional PON system. Thus, the MP-BPF can be realized by placing an ORDL at OLT as an optical subsystem. That is, the optical transmitter and receiver of an ONU are used for the conventional purpose of optical transmission between OLT and ONU, and used as the components of the MP-BPF at the same time. In the proposed system, modulated optical signal by an ONU is transmitted to OLT through the single-mode fiber and divided by an optical splitter. A half of the signal is fed to Rx for the U/S detection, and the other is sent back to the ONU via the ORDL. As the result, signals modulated on periodic passbands of

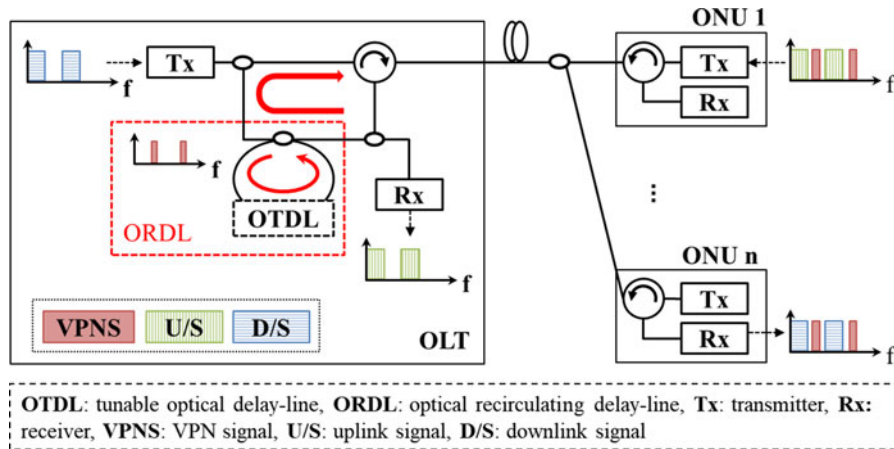


Fig. 2. Schematic of the proposed system.

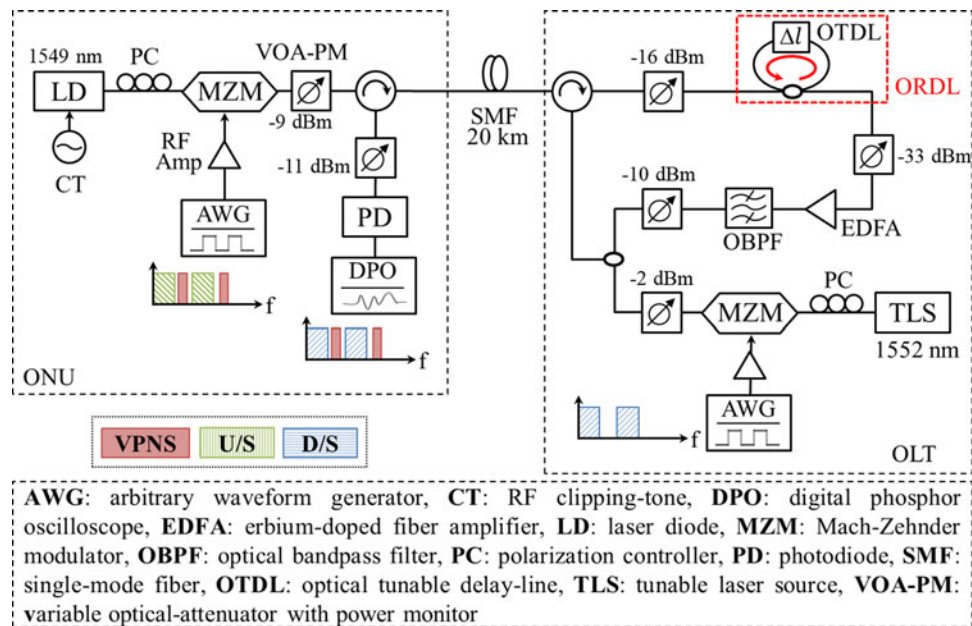


Fig. 3. Experimental setup.

the MP-BPF are delivered to ONU. Using this property, the all-optical VPN can be implemented by using the passband characteristics of MP-BPF for the VPNS transmission. On the other hand, the stopbands of MP-BPF are used for the conventional U/S, D/S transmission. As the result, the D/S and VPNS are separated in RF spectrum, and those can be detected with a single-PD. Also the DBA between VPN and conventional data can be implemented by using a tunable optical delay-line (OTDL), because the FSR of MP-BPF is determined by the sampling period of ORDL.

3. Experiments and Discussion

The proposed system was experimentally demonstrated as a proof of concept in 20-km single fiber loopback link as shown in Fig. 3. It was focused on verifying the CT effect on channel variations and transmission performance of VPNS and D/S with DBA function, because the U/S transmission is similar to general PON system. In order to overcome the MAI arisen from asynchronous transmission of VPSN and D/S, FBMC was used instead of OFDM. The real-valued FBMC signal

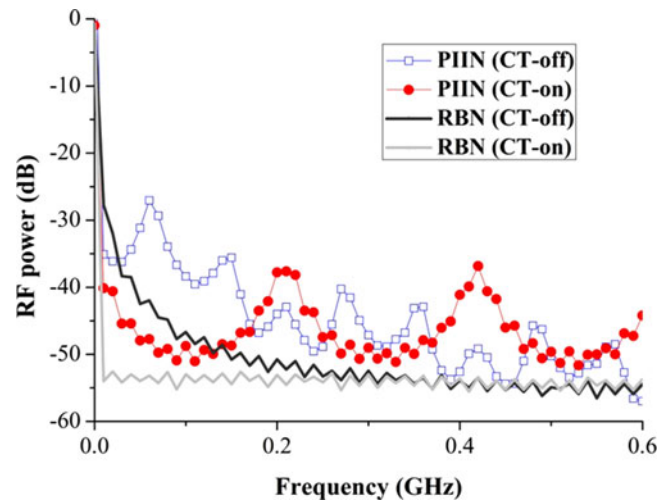


Fig. 4. Optical channel variations according to CT modulation.

of 2 GHz bandwidth was generated through MATLAB using Hermitian symmetry, and extracted by an arbitrary waveform generator (AWG). Using subcarrier allocation, VPNS was allocated on subcarriers corresponding to passbands of designed MP-BPF, while U/S and D/S are allocated on stopbands of the MP-BPF. The generated VPNS and U/S are electrically combined and optically modulated by a MZM biased at quadrature point, and the MZM output power was set to -9 dBm. It was fed to ORDL after 20-km transmission. An EDFA was used as an optical preamplifier, and the amplified spontaneous emission (ASE) noise was removed by an OBPF. The amplified VPNS signal was combined with D/S modulated on different optical wavelength of 1552 nm, and detected by a PD after 20-km optical transmission. It was evaluated through offline processing by using a digital phosphor oscilloscope (DPO). Some of the variable optical attenuators with power monitors (VOA-PMs) were used to control and monitor the optical power. The optical source for VPNS transmission was modulated by a CT in order to stabilize the optical channel from the PIIN and RBN. The channel variations, transmission performance of VPNS and D/S at different DBA scenarios were analyzed according to the applied CT frequency.

Fig. 4 shows RF spectra measured at PD after 20-km loopback transmission without modulated signal in order to observe the channel variations according to the CT in RF domain. The RBN variations were measured by bypassing the ORDL, and the Lorentzian-shaped RBN was suppressed by spectrum broadening effect of the CT modulation. Also the intensity fluctuation arisen from PIIN was removed, and the stable frequency response of MP-BPF could be achieved by the CT modulation, because it makes the coherence time of optical carrier becomes much smaller than sampling period of the ORDL as mentioned in Section 2. From the Fig. 4, it was verified that the optical channel related with coherence of optical carrier such as RBN and PIIN could be stabilized.

However the constant PIIN level could be varied by the applied CT frequency as described in Fig. 1(c). In order to verify this effect, the frequency responses of MP-BPF and the variations of noise level were measured according to the FSR and applied CT frequencies. Fig. 5(a) and (b) show frequency responses of MP-BPF at different FSR of 82 MHz and 210 MHz, respectively. The FSR was controlled by adjusting the delay length of ORDL. Due to the experimental limitations, an optical fiber and connector were inserted to ORDL in order to set the FSR to 82 MHz. As the result, Fig. 5(a) shows relatively low stopband attenuation compared to that of Fig. 5(b) for the FSR of 210 MHz owing to the increased optical loss which decides the recirculating tap-weight. However it could be improved by using an OTDL without tap-weight variations for the delay length control. As shown in Fig. 5(a) and (b), it has different noise level according to the CT frequency although the stable frequency responses of MP-BPF could be achieved by the spectrum broadening effect. The variations of noise floor were measured as varying the CT frequency from 5 GHz to 5.5 GHz as

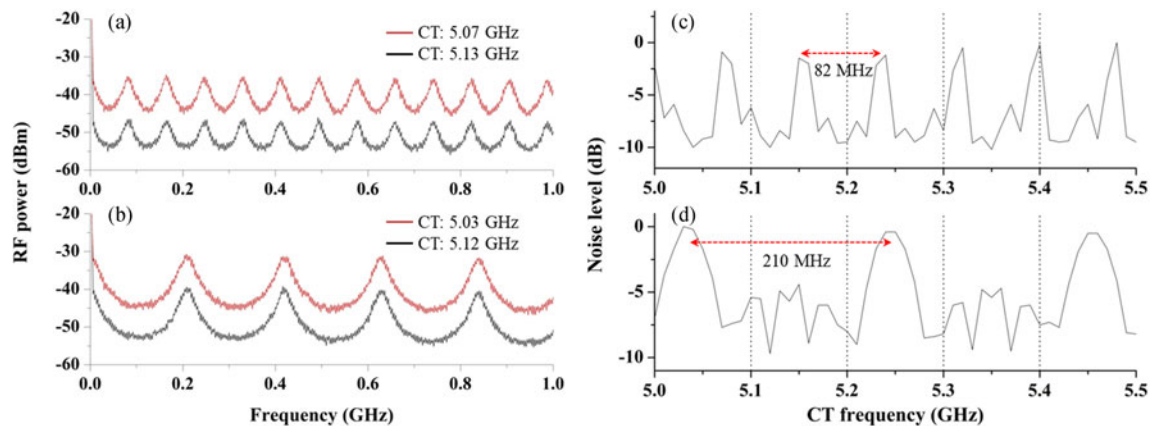


Fig. 5. Frequency responses at FSR of (a) 82 MHz and (b) 210 MHz, and noise level variations at FSR of (c) 82 MHz and (d) 210 MHz.

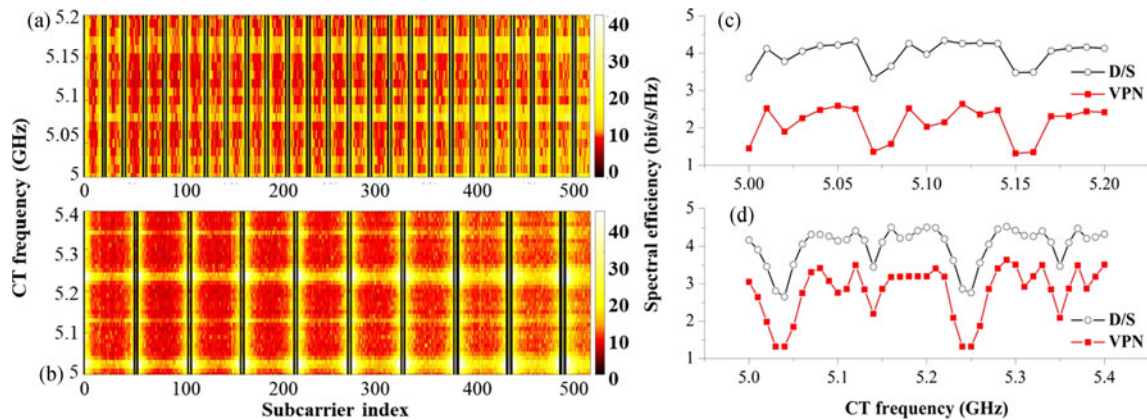


Fig. 6. Channel EVM variations at FSR of (a) 82 MHz and (b) 210 MHz, and spectral efficiency variations at FSR of (c) 82 MHz and (d) 210 MHz.

shown in Fig. 5(c) and (d). The results show periodic noise variations according to the applied CT frequency. When the FSR was set to 82 MHz, the noise level was varied with period of 82 MHz as shown in Fig. 5(c). Also, it was varied with period of 210 MHz, when the FSR was set to 210 MHz as shown in Fig. 5(d). That is, the periodic noise variations according to the CT frequency were corresponded to the filter FSR, and the maximum noise difference was about 10 dB. It is due to the fact that the optical beating noise becomes increased as the CT frequency becomes closer to the integer multiple of the FSR as described in Section 2.

This characteristic is reflected in the transmission performance as the SNR becomes varied according to the CT frequency and FSR of the MP-BPF. The Fig. 6(a) and (b) were measured channel error vector magnitude (EVM) of VPNS and D/S according to the CT frequency at different FSR of 82 MHz and 210 MHz, respectively. The number of FBMC subcarrier was 512, and VPNS was modulated on subcarriers corresponding to the passbands of the MP-BPF, while D/S was modulated on the stopbands. Two guard-subcarriers were used at both sides of VPNS subcarriers. Total signal bandwidth was 2 GHz. In the case of Fig. 6(a), 24 subcarriers were assigned to VPNS with cyclic interval corresponding to the FSR of 82 MHz, and the result shows EVM variations with period of 82 MHz for the applied CT frequency. In the case of Fig. 6(b), 9 subcarriers were assigned to VPNS, and the result also shows EVM variations with period of 210 MHz corresponding to the FSR. Based on the measured channel EVM, adaptive modulation was applied to investigate the achievable spectral efficiency (SE) with the target BER of 2×10^{-3} . As the channel variations were

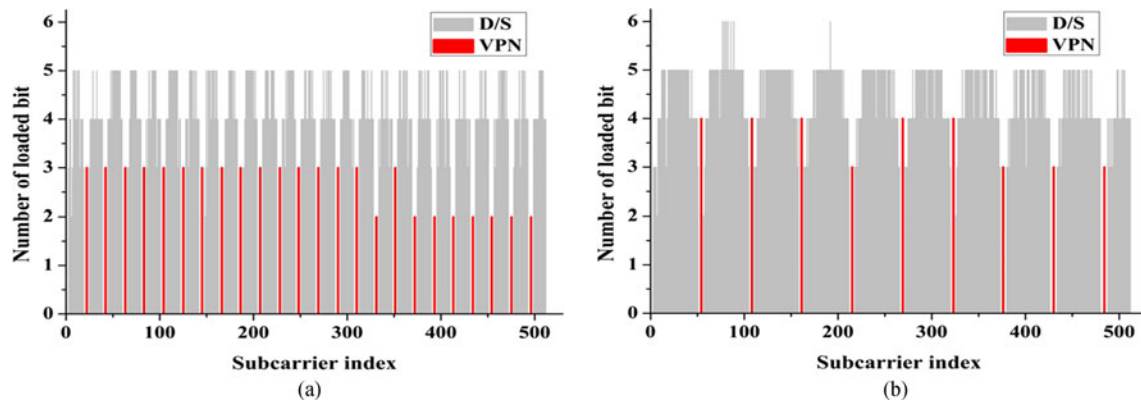


Fig. 7. Bit loading profiles according to different FSR of (a) 82 MHz and (b) 210 MHz.

reflected in the adaptive modulation, the SE was also varied with period corresponding to the FSR. When the FSR was set to 82 MHz as shown in Fig. 6(c), the SE of D/S and VPNS were varied from 3.34 to 4.34 and from 1.36 to 2.64, respectively. When the FSR was set to 210 MHz, the SE of D/S and VPNS were varied from 2.65 to 4.53 and from 1.32 to 3.64, respectively, as shown in Fig. 6(d). The results imply the transmission performance of the proposed system could be improved by adjusting the CT frequency according to the DBA condition. Fig. 7 shows bit-loading profiles when maximum SE was achieved at different FSR. In spite of the asynchronous multiple access, the VPNS and D/S could be simultaneously transmitted with only one guard-subcarrier due to the MAI robustness of the FBMC in both Fig. 7(a) and (b). In common, relatively a low number of bits were loaded on the boundary subcarriers between VPNS and D/S. It is due to the fact the U/S was not fully suppressed by limited stopband attenuation of MP-BPF, and it affect to D/S transmission. However it could be improved by reducing the recirculation-loss in the ORDL which decides tap weights of MP-BPF.

4. Conclusion

We proposed and experimentally demonstrated an MP-BPF based all-optical VPN supporting DBA in multi-carrier access PON system. The DBA was verified at different two DBA scenarios in 20-km single-fiber loopback link by adjusting a free spectral range (FSR) of the MP-BPF with corresponding subcarrier allocation. In order to stabilize the optical channel suffered from PIIN and RBN, CT was applied in the optical transmitter. Also, FBMC was used to reduce MAI arisen from the asynchronous transmission of multi-carrier signal in a single-PD operation. As stabilizing the optical channel by adjusting the CT frequency according to the DBA scenarios, spectral efficiencies of both VPN and D/S could be improve. Based on the experimental demonstrations, the proposed system is expected to be a feasible solution to implement all-optical VPN which is very demanding feature in future optical access networks, which accommodates full use of flexibility in bandwidth allocation, low system complexity, and wavelength tolerance.

References

- [1] N. Cvijetic, "OFDM for next-generation optical access networks," *J. Lightw. Technol.*, vol. 30, no. 4, pp. 384–398, 2012.
- [2] M. K. Hong, T. Shi, E. Tangdiongga, S. K. Han, and A. M. J. Koonen, "10-Gb/s transmission over 20-km single fiber link using 1-GHz RSOA by discrete multitone with multiple access," *Opt. Exp.*, vol. 19, no. 26, pp. B486–B495, 2011.
- [3] J. von Hoyningen-Huene, H. Griesser, M. H. Eiselt, and W. Rosenkranz, "Asynchronous signal reception in OFDMA-PON-uplink," in *Proc. Adv. Photon. Congr.*, Optical Society of America, 2013, presentation number: SP4D.2.
- [4] S. Y. Jung, S. M. Jung, H. J. Park, and S. K. Han, "Mitigation of timing offset effect in IM/DD based OFDMA-PON uplink multiple access," *Opt. Exp.*, vol. 23, no. 11, pp. 13889–13898, 2015.

- [5] N. Nadarajah, M. Attygalle, E. Wong, and A. Nirmalathas, "Novel schemes for local area network emulation in passive optical networks with RF subcarrier multiplexed customer traffic," *J. Lightw. Technol.*, vol. 23, no. 10, pp. 2974–2983, 2005.
- [6] Y. Tian, T. Ye, and Y. Su, "Demonstration and scalability analysis of All-Optical virtual private network in multiple passive optical networks using ASK/FSK format," *IEEE Photon. Technol. Lett.*, vol. 19, no. 20, pp. 1595–1597, Oct. 2007.
- [7] Y. Luo, F. Li, J. Liu, L. Gan, C. Lu, and P. K. A. Wai, "10-Gb/s All-Optical VPN in WDM-PON Using Injection-Locked Fabry–Pérot Laser Diodes," *IEEE Photon. Technol. Lett.*, vol. 26, no. 22, pp. 2299–2302, Nov. 2014.
- [8] X. Hu, P. Cao, L. Zhang, X. Jiang, Z. Zhuang, and Y. Su, "Flexible and Concurrent All-Optical VPN in OFDMA PON," *IEEE Photon. J.*, vol. 5, no. 6, pp. 7902707–7902707, Dec. 2013.
- [9] C. Zhang, J. Huang, C. Chen, and K. Qiu, "All-optical virtual private network and ONUs communication in optical OFDM-based PON system," *Opt. Exp.*, vol. 19, no. 24, pp. 24816–24821, 2011.
- [10] C. H. Kim, S. Y. Jung, S. M. Jung, and S. K. Han, "All-Optical virtual private network in OFDM-PON using microwave photonic filter," *IEEE Photon. Technol. Lett.*, vol. 28, no. 24, pp. 2830–2833, Dec. 2016.
- [11] J. Capmany, B. Ortega, and D. Pastor, "A tutorial on microwave photonic filters," *J. Lightw. Technol.*, vol. 24, no. 1, pp. 201–229, 2006.